

Retraction

Retracted: Multi-Objective Optimization Algorithm and Preference Multi-Objective Decision-Making Based on Artificial Intelligence Biological Immune System

Juan Bao; Xiangyang Liu; Zhengtao Xiang; Gang Wei

IEEE Access

10.1109/ACCESS.2020.3020054

<p>Notice of Retraction</p> <p>J. Bao, X. Liu, Z. Xiang, and G. Wei, “Multi-objective optimization algorithm and preference multi-objective decision-making based on artificial intelligence biological immune system,” *IEEE Access*, vol. 8, pp. 160221–160230, 2020, doi: 10.1109/ACCESS.2020.3020054.</p> <p>After careful and considered review by a duly constituted expert committee, this article was retracted owing to irregularities in the peer review process, including acceptance for publication without the minimum number of independent reviews required by IEEE.</p> <p>The authors were contacted about the retraction and did not dispute it.</p>

Received August 7, 2020, accepted August 24, 2020, date of publication August 31, 2020, date of current version September 14, 2020.

Digital Object Identifier 10.1109/ACCESS.2020.3020054

Multi-Objective Optimization Algorithm and Preference Multi-Objective Decision-Making Based on Artificial Intelligence Biological Immune System

JUAN BAO¹, XIANGYANG LIU¹, ZHENGTAO XIANG², AND GANG WEI^{1,3} 

¹Center of Health Administration and Development Studies, School of Public Health, Hubei University of Medicine, Shiyan 442000, China

²School of Electrical and Information Engineering, Hubei University of Automotive Technology, Shiyan 442002, China

³The Affiliated People's Hospital of Hubei University of Medicine, Shiyan 442000, China

Corresponding author: Gang Wei (weddy_0926@126.com)


This work was supported in part by the Key Research Center for Humanities and Social Sciences in Hubei Province (Hubei University of Medicine) under Grant 2019ZD003, and in part by the Start-up Foundation of Hubei University of Medicine under Grant 2019QDJRW02.

ABSTRACT The operating mechanism of the biological immune system is often used for the development of intelligent technology. This research introduces the multi-functional optimization algorithm of the biological immune system into the VR image segmentation, and proposes a multi-purpose VR image segmentation method with more stable and better segmentation performance. In order to combine it with the characteristics of the VR image itself, a complementary feature extraction method combining filters and gray-level symbiosis probability is used. In addition, in order to enable the algorithm to solve the segmentation problem of huge pixel images, the best solution is found through communication and exchange between subgroups. Use the excellent genes of the memory genes as the imported genes and introduce the inferior individuals to strengthen the mining of the best solution of Pareto at the boundary of the impossible field. In order to verify the performance of the algorithm, 3 synthetic texture images and 2 actual VR images are used, 8 constrained targets and 4 unconstrained target benchmark functions are selected to test the optimization function of PCMIOA. Multipoint parallel search uses two different search schemes, local and global. In this way, the domain value of the highest value can be searched globally, and the local best solution can be searched at the same time, realizing the global search mechanism. The relatively satisfactory target value is 98.25, and the deviation between the corresponding solution and the ideal solution is 0.093. The results of the research show that Multi - objective optimization algorithm is an excellent demonstration of the diversity of Pareto-oriented methods and solutions. Compared with the previous prediction methods, this method has higher prediction accuracy and robustness. The choice of decision makers can be taken into consideration, and subjective willfulness can be reduced to make decision results more realistic and reliable.

INDEX TERMS Artificial intelligence, biological immune system, multi-objective optimization algorithm, preference multi-objective decision-making, VR panorama.

I. INTRODUCTION

The biological immune system is a high-intelligence technology system that is parallel and dispersed and can adaptively process information, and can provide real-time information [1]. It continuously utilizes, enriches system resources, and continuously develops and improves existing artificial immune models [2]. Its theoretical and applied

The associate editor coordinating the review of this manuscript and approving it for publication was Zhihan Lv .

research has become an important research content and mainstream development applied to artificial immune system theory and artificial intelligence. The computational complexity of multi-objective optimization algorithms is very high, but it reflects the diversity and distribution of images from a macro perspective, and more appropriately represents the internal relationships between images, which play an evolutionary role in image changes [3].

Therefore, the multi-objective optimization algorithm can improve the overall diversity and the distribution of Pareto

optimal solutions. Numerical calculations are carried out through two standard test function algorithms. Based on the classic multi-objective selection algorithm, the theory of multi-objective selection algorithm is introduced and compared with genetic algorithm, and the conclusion that the two algorithms can be used for reference is drawn. In this research, we will find a new entry point, design a new improvement plan, and design an improved multi-objective selection algorithm based on an improved selection operator.

The biological immune system promotes technological progress. Saileela discussed ideas related to computability, algorithmic information theory, and software engineering [4]. Theoretical computer science provides concepts in translation practice from computing to molecular biology to translation. These concepts provide a means for hierarchical organization, thereby blurring the previously clear boundaries between concepts such as matter and life, or blurring the boundaries between tumor types [5]. His research process lacks concrete practical steps [6]. Qian proposed an immune optimization algorithm based on a biological immune system model to solve multi-objective optimization problems with multi-peak nonlinear constraints. First, divide the initial population into viable non-dominated population and infeasible dominated population. Feasible non-dominated individuals focus on the proposed affinity design method, exploring non-dominated frontiers through cloning and hypermutation, while infeasible dominated individuals are utilized and improved by simulating binary crossover and polynomial mutation operations. Then, in order to speed up the convergence speed of the algorithm, the transformation technique is applied to the merged population of the above two offspring populations. Finally, a crowded comparison strategy was adopted to create the next generation of population. In the numerical experiments, a series of benchmark-constrained multi-objective optimization problems were considered to evaluate the performance of the proposed algorithm and compared it with several latest algorithms [7]. His research process is too cumbersome and the focus is not strong enough [8]. By ignoring the relatively weak direct immune activation of tumor cells, the previous tumor-immune interaction model is simplified, and the model can still retain the basic dynamic characteristics of the original model. Yu believes that since the immune activation process is not instantaneous, a delay time is now used to activate the effector cells (EC) of helper T cells (HTC) into the model. In addition, for two parameters, he studied the activation rate of HTC on EC and the HTC stimulation rate of the presence of identified tumor antigens on the two parameters, and studied the stability and instability of the equilibrium state of tumor existence in the delayed induction system. area. His research process lacks specific data [9]. The artificial immune system (AIS) is inspired by the biological immune system (BIS) and exhibits many interesting aspects and intelligences, including self-learning, self-adaptation, self-regulation, and self/non-self detection capabilities. Saurabh proposed “efficient active artificial immune system based on anomaly detection and prevention

system” (EPAADPS), which embodies immune characteristics to distinguish self from non-self, seeking to identify and prevent novel, invisible abnormalities. Negative selection algorithm (NSA) is the key concept of AIS and is used for anomaly detection. EPAADPS is not accurate enough to be practical [10].

Multi-objective optimization algorithms are widely used in the field of computational intelligence to analyze the theory of multi-objective optimization algorithms [11]. There is very little traditional research work. Therefore, this research is similar to the research of genetic algorithms, using convergence research methods to study multi-objective selection attributes and optimization problems the multi-objective optimization algorithm in the estimated solution and the sufficient conditions for convergence to the global optimal solution. This paper will further study the random convergence characteristics of general multi-purpose optimization algorithms, that is, the upper limit of evolutionary algebra that the algorithm needs to find the best solution under a certain fixed probability. Comparing the upper limit of the evolutionary algebra required to find the optimal solution under a fixed probability with the upper limit of the genetic algorithm, the decision-making optimization scheme can be further derived [12].

II. BIOLOGICAL IMMUNE SYSTEM

A. PRINCIPLE OF ARTIFICIAL IMMUNE ALGORITHM

The basic principle of artificial immune algorithm is to gradually realize antibody optimization through the process of antibody and antigen binding, antibody cloning, mutation, selection, and memory. Algorithms can be used to solve multi-objective optimization problems, antigen can also be mapped to the objective function of the optimization problem, or antibodies can be mapped to an executable solution to the optimization problem. The degree of agreement between the executable solution and the objective function can be expressed by the affinity between the antigen and the antibody. By calculating genetic and variable antibodies that can promote better survival rates, the diversity of executable solutions due to the affinity between antibodies can be confirmed, and solutions for executable memory units can be obtained. Using this scheme, you can prevent similar executable solutions from being generated [13]. While speeding up the search for the global best solution, if the same problem occurs again, you can solve the most suitable problem, so the most suitable solution can be Solve immediately [14].

Enter the objective function and constraint conditions as the antigen input, and set the initialization parameters related to the initial overall size. When solving the optimization problem for the first time, the randomly generated m can be used as the actual coded individual A of the first population. When solving the problem, if the same problem has been solved, first extract the (optimized variable experimental data) m from the immune memory database of the specific immune memory unit, and form the initial antibody data according to the increase in the amount of remaining

probability variables [15-17].

$$f_k = \frac{1}{2} \sum_{k=1}^m \left(g_2 \left(\sum_{j=1}^{s_1} w_{1jk} g_1 \left(\sum_{i=1}^r w_{2j} + \theta_{1j} \right) + \theta_{2k} \right) - y_{dk} \right)^2 \quad (1)$$

Among them, θ_{1j} and θ_{2k} are the threshold vectors of the hidden layer and the output layer [18], [19].

The mechanism of cell cloning and memory cell acquisition mainly lies in the differentiation of immune cells. In cell differentiation, some cells will evolve into memory cells, and other cells will replicate most of the asexual reproductive system (ie, clones). These cloned cells participated in evolution and evolved into metamorphic cells. This mechanism is reflected in the algorithm. The memory unit is a better solution obtained when the algorithm evolves to the current totality, and these solutions will gradually be replaced by better solutions. The function of the memory unit is to solve the same or similar problems for the initial individual. This helps improve the performance of searching for the best solution. The clonal evolution of immune cell proliferation (ie, replication of candidate solutions) provides opportunities to detect better solutions and strengthens the local search function of the algorithm [20].

B. MULTI-OBJECTIVE OPTIMIZATION ALGORITHM

There are many multi-benchmark decision-making problems in real life, and finding the best solution that satisfies decision makers is the ultimate goal of solving these problems. However, in general classical multi-function optimization algorithms, a series of optimal solution sets that approximate Pareto globally are always detected [21]. Therefore, the decision-maker must choose a satisfactory solution, which not only increases the complexity of the algorithm itself, but also increases the difficulty of the decision-maker's solution. In addition, these classic algorithms cannot simply solve the above-mentioned high-dimensional multi-functional optimization problem. This is because as the target size increases, non-optimal solutions based on Pareto's advantage also increase exponentially. As the selection pressure of the algorithm weakened rapidly, it could not be repeated and the convergence failed. Combining the preference information of decision makers with problem investigation is a good feasible solution to this problem [22]. In order to distinguish it from the traditional multi-objective optimization algorithm, this is usually called the priority multi-project table optimization algorithm. The performance index is obtained by minimizing the average square deviation between the measured value and the model estimated value [23].

$$\begin{aligned} \min (E^2) &= \sum_{k=1}^N [y'(k) - y(k)]^2 \\ &= \sum_{k=1}^N \left[y'(k) - \sum_{i=1}^M p_i F_i(x) \right]^2 \quad (2) \end{aligned}$$

Among them, $y(k)$ is the measured value, N is the number of data points.

C. PREFERENCE FOR MULTI-OBJECTIVE DECISION MAKING

Various setting mechanisms are actually based on reference points and reference vectors. In addition, one of the general principles of these methods is that, regardless of whether the priority solution is around or near the reference point, the angle between the priority solution and the reference vector is actually smaller than the angle between the non-priority solution and the reference vector. The reference direction is a priority mechanism based on the reference direction, and the reference vector is a prescribed reference direction. For the priority mechanism based on the reference point, the reference vector is composed of a line between the origin and the reference point. Therefore, inspired by the above ideas, we have carefully designed an angle priority selection mechanism. This not only requires calculating a part of the scaling formula used in other priority mechanisms, but also requires less reference information [24]. The new priority mechanism is shown below.

$$Angle(a, r) = \arccos \left(\frac{a \cdot r}{|a| * |r|} \right) \quad (3)$$

The vector a is obtained by connecting each x to the starting point, and the vector r indicates the search direction of the load setting information. The angle allocated by the above formula is regarded as the selection criterion of the algorithm solution in the optimization process. Therefore, this method can not only increase the selection pressure of knowledge, but also cleverly combine the preference information of decision makers to guide the search to the algorithm of the preference domain [25], [26].

D. INTELLIGENT CONTROL BASED ON IMMUNE ALGORITHM

Intelligent control is the second-generation control theory that has been gradually developed since the 1990s. Intelligent control does not require an accurate object model, so it is widely used in self-adaptation, self-organization and self-learning, and complex system control. In the process of intelligently controlling applications, human knowledge, experience, and thinking patterns have a great influence on the choice of control methods and control effects. For example, the division of fuzzy theory domain, the decision of fuzzy rules, the network structure of neural network, the form of neuron transfer function, and the determination of the weight of neuron connection in fuzzy control all depend on the designer's experience. Improper setting will seriously affect the control effect [27], [28]. However, in actual situations, especially for complex objects, human knowledge and experience will be limited and often become unilateral problems. Therefore, in order to effectively complete the intelligent control tasks of complex objects, it is particularly important to improve the self-learning and self-organization capabilities of the machine [29]. The model evaluation module can obtain the prediction error of the model by comparing the measured data with the estimated value of the model, evaluate the model, and control the system according to the evaluation

result to further determine the module. In order to prevent erroneous evaluation results due to data interference, a certain time model is used as the evaluation criterion [30].

$$E_c = \frac{1}{L} \sqrt{\sum_{i=0}^{l-1} [y(k-i) - y_m(k-i)]^2 + y_m(k-i)} \quad (4)$$

Here, L is the evaluation time zone. E is the estimated average square error of the time domain model [31], [32].

The purpose of group distance selection is to calculate the density of individuals, select relatively sparse individuals, improve the diversity of individuals, and make individuals evenly dispersed. Sort the population in ascending order according to the target value of each dimension, and finally get the dense value of the individual [33], [34].

$$Crowd [i]_d = Crowd [i] + \frac{Crowd [i+1]_m - Crowd [i-1]_m}{f_m^{\max} - f_m^{\min}} \quad (5)$$

Here, $Crowd [i]_d$ represents the maintenance target value of MTH, f_m^{\max} and f_m^{\min} are the two extreme values of the overall MTH maintenance target. The artificial immune system is suitable for intelligent control. It adopts the adaptability, self-learning, self-organization ability and immune optimization method of the artificial immune system and other powerful robust functions to solve the best design of intelligent control, and design the intelligent control system for intelligent control. Improved the difficulty of intelligent control, improved the effective control effect, and achieved remarkable results [35].

E. VR TECHNOLOGY

Based on computer technology, VR integrates graphic resources, digital resources, and other information resources to form interactive visual 3D dynamic vision and tactile animation. Related terminal devices are used to identify VR virtual reality scenes, and bring experience immersion to the experience [36]. Nowadays, the application of VR technology has a wide range of fields, and it has the advantage of merging with various technologies. For example, the film and television industry, education industry, marketing industry, entertainment industry and construction industry have become the new preferences of market consumption, and gradually formed a new market form [37], [38]. The creative and experiential technology of VR is considered to play an important role in people's future life, bringing new experiences to people's life, work, and study [39].

In the virtual reality scene, the detailed functions of the 3D model surface are expanded, and the richer the surface details, the higher the performance [40]. However, the richer the detailed functions of the surface, the more system resources the model occupies. Therefore, in order to provide theoretical support for model mapping, theoretical research on texture mapping is required. In virtual reality scenes, in order to make the three-dimensional model of the object more realistic, the detailed functions of the surface of the object model are usually very complicated, the number of model grids is greatly increased, the system delay of most operating resources and

TABLE 1. Corresponding 5 Algorithms.

Index	1	2	3	4	5
Algorithm	NSGAI	MOEA	NNIA	SPEA2	NNIA+IED

other machines related to the same phenomenon occur. With texture mapping technology, a detailed image with object characteristics can be mapped to the surface of the object, so the object has the detailed characteristics of the image. In other words, a model with a small number of grids shows the characteristics of the model. The number of grids can be increased to reduce the resource consumption of the system and improve the operating speed of the system [41], [42].

III. MULTI-OBJECTIVE OPTIMIZATION ALGORITHM DECISION EXPERIMENT

A. EXPERIMENTAL PARAMETER SETTING AND EVALUATION INDEX SELECTION

This study compared NSGAI, MOEA, NNIA, SPEA2, NNIA+IED, and the corresponding five algorithms are shown in Table 1. Based on NSGAI, EMOEA and SPEA2, the online evolution group size is 90, and the outer group size is 80. Based on NNIA and NNIA+IED, the collective size of antibodies is 90, and the collective size of non-optimal active antibodies is 30. In these five algorithms, the evolutionary algebra is set to 400. The crossover probability is set to 0.8, and the mutation probability is the inverse of the number of variables.

The existing measurement standards mainly use the reference set of the most suitable Pareto solution. On the one hand, if the curvature in front of the best Pareto of the problem changes greatly, it is generally difficult to obtain the best reference solution of uniform distribution. At the same time, the number of Pareto best solutions has a great influence on the final evaluation index, and the accuracy of the evaluation index is often limited by the number of best reference solutions. Therefore, this study used a non-reference set of measurement standards. Use the coverage between two solution sets to measure the dominant relationship between the solutions obtained by different algorithms, and use the uniformity of solution distribution to measure the interval. The distribution width of the solution is used to measure the maximum distribution.

B. COMPARATIVE EXPERIMENT SETTINGS

In the comparative experiment, the end condition of all preferred multi-objective evolutionary algorithms based on reference points is the maximum evaluation time of the test problem. Due to the different difficulty of convergence for different dimensional test problems, this study sets the maximum evaluation time for different dimensional test problems. The maximum number of evaluations for the ZDT series of test functions is $200 \times N$. The maximum number of evaluation questions for the DTLZ and WFG series is $200 \times N$.

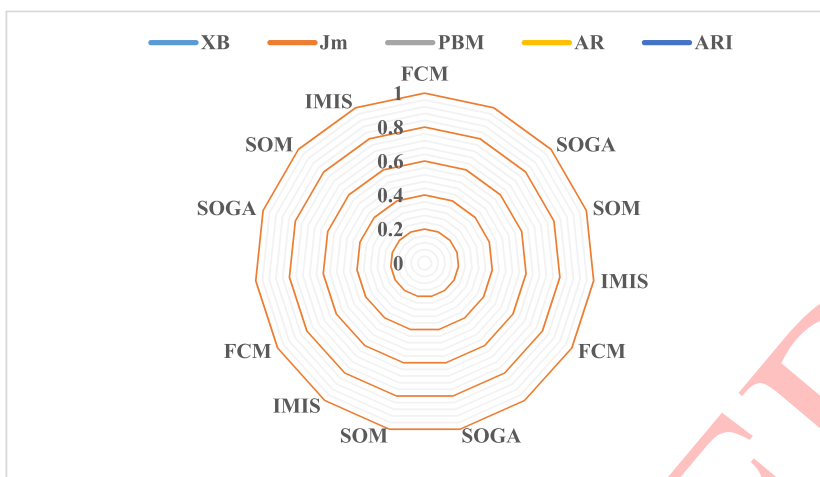


FIGURE 1. Segmentation results of four types of synthetic texture images.

The maximum evaluation time of 5D DTLZ series test questions is $300 \times N$, and the maximum evaluation time of WFG series test questions is $400 \times N$. The maximum number of evaluations for the 8-dimensional DTLZ and WFG series of test questions is $700 \times N$. The maximum number of evaluations for 10-dimensional DTLZ and WFG test questions is $900 \times N$. N is the size of the population, and the value is set to 90.

C. COMPARISON OF EFFECTS ON SCH, DEB AND ZDT ISSUES

This study compares the performance of AMOSA, NNIA, NSGAI and PESAI, which are SAIA and other four traditional multi-functional optimization algorithms. All algorithms were executed 20 times for each test question. For SAIA and AMOSA, T_{mx} is 100 and the annealing ratio is 0.9. NSGAI and PESAI simulate binary crossover and polynomial fluctuations. The archive size of AMOSA is 100. In the case of NNIA and NSGAI, the overall size is 90. In the case of PESAI, the total external size is 80, the archive size is 100, and the number of super units in each dimension is 19.

D. FEATURE EXTRACTION

Considering the feature extraction method comprehensively, this study uses Gabor filtering and gray-level symbiosis probability to extract fused complementary features. The former can better extract intermediate frequency feature information, but is sensitive to noise. The gray-level symbiosis probability can stably obtain the high-frequency details of the image. The pixel quantization level is 30, the local window size is 8×8 , the distance between pixels is 2, and the direction is set to $10^\circ, 30^\circ, 75^\circ, 120^\circ$. When the area is changed, the window size of the structural element is 4×4 .

E. PERFORMANCE VERIFICATION OF MULTI-OBJECTIVE OPTIMIZATION ALGORITHM

In order to further verify the performance of the multi-objective optimization algorithm, the optimized performance is compared with the performance of SPEA2 and NSGA2. The evolutionary collective size of the artificial immune multi-objective system is $N=20$, the outer collective size

is $NM=80$, and multiple clones $CS=6$. SPEA2 parameters are the same as the original parameters. In other words, the overall sample size is initialized to 90, the external overall size is initialized to 80, the probability of change is set to 0.2, and the crossover probability is set to 0.7. The change probability of NSGA2 is $1/n$, N is the number of determining variables, and the crossover probability is 0.8. In order to match the calculation amount of the three algorithms, the iteration stop condition of the three algorithms is 90 generation evolution.

IV. MULTI-OBJECTIVE OPTIMIZATION ALGORITHM DECISION ANALYSIS

A. MULTI-OBJECTIVE OPTIMIZATION ALGORITHM DECISION RESULT ANALYSIS

The segmentation results of the four types of synthetic texture images are shown in Figure 1. The figure shows that SOGA and SOM have many wrong spot divisions in local areas, IMIS and HMTSeg have achieved better segmentation results in the regional consistency of the image, followed by SCE. However, considering the distinction of regional boundaries, SCE and IMIS have achieved relatively good results, and the middle part of the segmentation results of HMTSeg is incorrectly divided. For the segmentation of four types of texture images, IMIS, HMTseg and SCE obtain the optimal statistical mean and variance of AR and ARI indicators. Although FCM obtains relatively good primary division results, its statistical mean is unstable. SOGA uses the XB index as a genetic image segmentation algorithm to optimize the objective function, and it obtains the optimal objective function value for this index. While FCM and SOM are single-objective image segmentation algorithms that optimize the Jm index with different mechanisms. They also achieve the smallest Jm index value, but none of the three algorithms can achieve better PBM, AR and ARI index values. It is worth paying special attention to that although IMIS cannot obtain the optimal XB and Jm values, when these two indicators are optimized at the same time, the optimal PBM, AR and ARI values are obtained. It shows that the optimal image division method does not exist in the extreme points of the two

TABLE 2. Results of FCM, SOGA, SOM, MIS used to segment TWO, FOUR and FIVE types of synthetic texture images, respectively.

Image	Algorithm	Evaluation index				
		XB	Jm	PBM	AR	ARI
Texture1	FCM	0.126(0.002)	297.68(0.021)	1.97(0.08)	99.40(0.001)	99.4(0.01)
	SOGA	0.114(0.002)	364.50(0.022)	1.54(0.06)	99.39(0.001)	99.3(0.01)
	SOM	0.143(0.001)	265.76(0.021)	1.45(0.08)	99.37(0.002)	99.3(0.002)
	IMIS	0.106(0.002)	280.39(0.022)	1.55(0.07)	99.32(0.001)	99.9(0.01)
Texture2	FCM	0.224(0.016)	111.98(8.32)	0.71(0.05)	86.44(13.4)	98.7(0.22)
	SOGA	0.243(0.013)	155.79(9.50)	0.72(0.26)	81.12(14.8)	98.7(0.02)
	SOM	0.409(0.014)	108.25(8.40)	0.47(0.08)	76.32(12.2)	86.4(13.4)
	IMIS	0.243(0.01)	125.83(5.91)	0.87(0.01)	98.62(0.02)	81.1(14.8)
Texture3	FCM	0.7209(0.4)	98.21(21.03)	2.75(0.43)	84.83(21.56)	0.86(0.01)
	SOGA	0.129(0.01)	110.16(9.66)	2.69(0.389)	86.69(6.34)	0.89(0.01)
	SOM	0.16(0.028)	103.94(1.42)	2.35(0.37)	77.17(3.05)	0.75(0.014)
	IMIS	0.19(0.025)	102.19(1.12)	3.29(0.17)	96.45(2.19)	0.91(0.028)

optimization goals, but in their compromised parts, and only the multi-objective optimization algorithm can find the solution of the compromised parts of different indexes. Therefore, using two mutually exclusive objective functions to guide the solution search process can expand the search range and find more novel solutions, which is conducive to problem solving.

The results of FCM, SOGA, SOM, MIS used to segment two, four and five types of synthetic texture images are shown in Table 2. It can be seen from the table that the five comparison algorithms used in this study have obtained better segmentation results for the two types of synthetic texture images, which shows that the feature extraction method used in this study can better capture the texture information in the image. Greatly simplify the image segmentation process. It shows that FCM and SOGA have achieved the best statistical accuracy measurement indicators and ARI indicators, followed by MIS. In addition, the algorithm in this research has stable partitioning results, and its performance is more stable than FCM. For segmented images of two types of textures, if an appropriate texture feature description method is used, then due to the small number of categories, the traditional FCM and SOGA can achieve relatively satisfactory results. The advantage of the algorithm in this research is to deal with complex image sample distributions. And the image segmentation problem with a large number of categories. It can reflect that the minimum average calculation times is 90 times, the maximum is 3785 times, the minimum first arrival time is 13, and the maximum is 541, indicating that the selection of parameters in this area easily affects the search speed of the algorithm, so this area is not desirable. In addition, when $\sigma > 0.4$, the effect of σ on the convergence, first arrival time and average calculation times of the algorithm is quite obvious. Divide the time into 6 segments, and the u in each segment can only take 3 values. For this problem, the worst value found by Opt-AiNet is 0.00730, while the HOpt-AiNet with local optimization operator is 31.955. The worst value found is greatly improved, and the computational cost is only 2.56 times the original. The average value and worst value found by HOpt-AiNet using sequential refinement strategy are better than HOpt-AiNet, but the average number of evaluations is saved by 40.33%, and the average calculation time is saved by 61.98%.

B. PRUNING SCALE ANALYSIS

The pruning scale s is very important for SAIA in terms of time cost and diversity index. This study mainly discusses the influence of the pruning scale on the performance of the algorithm in the simulated annealing iteration. Figure 2 shows the relationship statistics of SAIA's performance in diversity index and time spent in the process of pruning scale from 1 to 50. It can be seen from the figure that in terms of diversity indicators, although the performance of the algorithm for the DTLZ1 problem fluctuates, in general, the smaller the pruning scale, the better SAIA's performance in diversity indicators. In addition, in terms of time cost, the smaller the pruning scale, the greater the time cost. However, when the pruning scale is greater than 10, the decreasing speed of the time cost becomes slower and almost tends to a constant constant value. In short, the pruning scale has a relatively large impact on the performance of SAIA in terms of diversity indicators and time spent. Finally, it can be concluded that in terms of convergence index and uniformity index, function evaluation is very important for SAIA performance at this time, while the clone scale does not have such a big impact. In terms of time spent, the soft cap and pruning scale have a greater impact on SAIA performance. In this case, the objective function is composed of 200 sub-objective functions, and we divide it into 4 groups, each group contains 50 sub-objective functions, and then obtain 4 sub-objective functions that are accumulated, and then use the immune network optimization algorithm (INOA) For optimization, a satisfactory target value of 98.25 is obtained, and the deviation between the corresponding solution and the ideal solution is 0.093. The process of searching the maximum value of the algorithm and the process of searching the optimization with INOA in the case of undecomposed objective function are obtained. From the graphs and search results, decomposing the objective function and then using INOA to find the optimization has great advantages. This demonstrates the effectiveness of INOA in solving high-dimensional complex multi-peak optimization problems.

In order to test the performance of the algorithm CP-NSGA-II under different reference point positions, this study sets three different positions for the ZDT and DTLZ series of test functions (infeasible region (u), feasible region

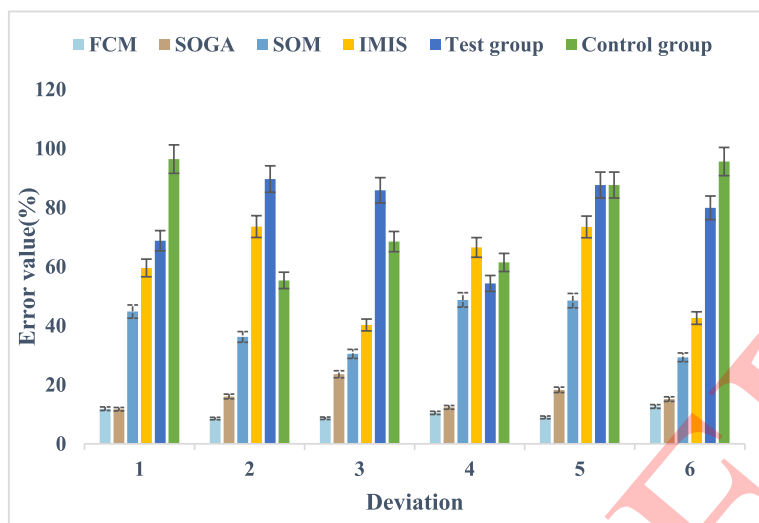


FIGURE 2. The relationship between SAIA's performance in diversity indicators and time spent in the process of pruning scale from 1 to 50.

TABLE 3. Reference point settings for ZDT test set and 3D DTLZ test problems.

Test Problem	Reference point position setting		
	Infeasible area	Feasible region	Near real POF
ZDT1	(0.10,0.20)	(0.40,0.55)	(0.30,0.45)
ZDT2	(0.10,0.10)	(0.70,0.80)	(0.60,0.64)
ZD T3	(0.10,0.20)	(0.40,0.50)	(0.24,0.28)
DTLZ1	(0.10,0.20,0.10)	(30,0.8,0.25)	(0.12,0.31,0.68)
DTLZ2	(0.20,0.50,0.60)	(70,0.8,0.50)	(0.50,0.77,0.38)
DTLZ3	(0.20,0.50,0.60)	(70,0.8,0.50)	(0.50,0.77,0.38)

(a), real POF (o) Reference points, ZDT test set and reference point settings for 3D DTLZ test problems are shown in Table 3. From the data in the table, it can be seen that the comprehensive performance of CP-NSGA-II is better than other comparison algorithms in the comparison experiment between the 2D ZDT test set and the 3D DTLZ and WFG test set. For g-NSGA-II, although a solution set with good convergence can be obtained, due to the different position of the reference point, the obtained solution set is either too extensive or too concentrated. It is in ZDT2 (concave) and ZDT4 (convex).) On the test problem, because the reference point is in the infeasible region and far away from the real POF, the preference solution set obtained by g-NSGA-II is too extensive. When the reference point is set on the real POF, the solution set obtained by g-NSGA-I is too concentrated, and almost all preferred solutions converge to the location of the reference point. g-NSGA-I performs well on the 3-dimensional WFG test problem, and it can be seen that g-NSGA-II is stable in convergence. For r-NSGA-II, although it has a good performance on the 3D DTLZ4 test problem, when the reference point is set in the feasible region, r-NSGA-II is due to the preference of individuals being used by other algorithms when calculating R-HV. Dominated by the solution set of DTLZ2 and DTLZ4, the R-HV value is a null value. When the reference point is set on the feasible region, r-NSGA-I basically does not converge to the true POF. In addition, when the reference point is set on the real POF,

the solution set of r-nsga-i is affected by the reference point, and the solution set converges to one point, which further indicates that the performance of r-nsga-ii is unstable due to the setting of reference points.

C. SECONDARY RESPONSE OF HYBRID OPTIMIZATION ARTIFICIAL IMMUNE NETWORK

In order to investigate the impact of the secondary response on the performance of the algorithm, the performance difference algorithm between HOpt-AiNet* and HOpt-AiNet2 with no secondary response and HOpt-AiNet2 with the secondary response was investigated by perturbing the instance parameter Q slightly. The running result of the secondary response is shown in Figure 3. The parameter of HOpt-AiNet* in the figure is Q+AQ. In the figure, HOpt-AiNet2 means: first take the value Q and use HOpt-AiNet* for optimization. At this time, some of the antibodies obtained will be stored in the antigen library, and then adjust the parameters to Q+4Q, and then call HOpt-AiNet*, the parameters are N=5, G=Q+2Q will take 4 different values. From the data in the figure, it can be seen that compared with the algorithm without the secondary response mechanism, the optimal value of the result of the algorithm with this mechanism does not decrease, but the number of evaluations and calculation time are greatly reduced, and the average number of evaluations is saved. It is 88.34%-89.11%, and the average calculation time is saved 70.09%-71.59%. It shows that the

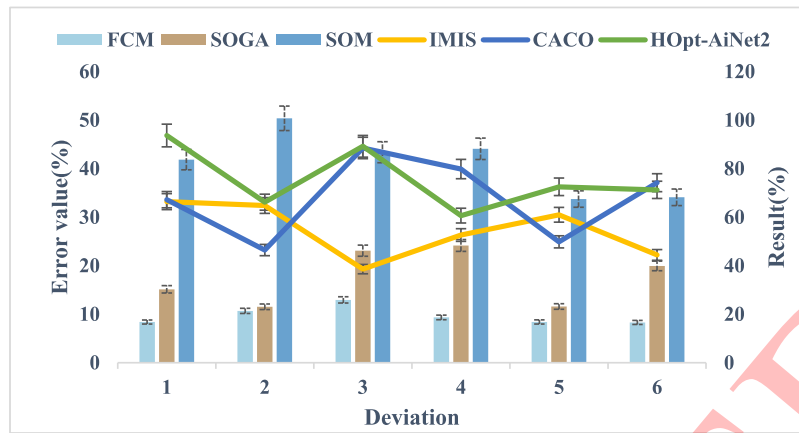


FIGURE 3. The running result of the secondary response.

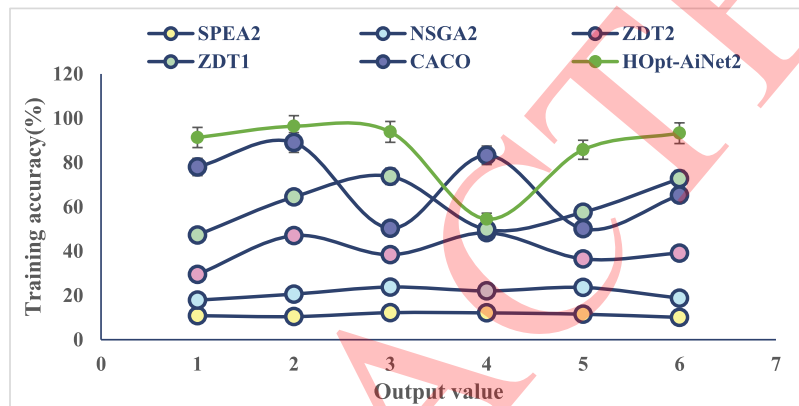


FIGURE 4. Comparison of the learning output value of the multi-objective optimization algorithm model and the corresponding actual output value and the relative error of the corresponding output value.

secondary response mechanism is very effective for process optimization with slight adjustment of model parameters, and is suitable for many practical problems. In fact, a better initial feasible solution is conducive to the algorithm to find the optimal solution faster. The secondary response mechanism is intended to make the initial feasible solution near the optimal solution based on the original work, thereby improving the efficiency of the algorithm. The continuous ant colony algorithm (CACO) is used to solve the problem, and the crossover and mutation in the genetic operation are introduced into the ant colony algorithm, thereby constructing the continuous ant colony algorithm CACO suitable for continuous problems. Its time segment number $n=4$, the control variables are linear functions, and static functions are used to deal with the constraints of state variables. Among the results obtained by running 25 times, the best is 20357, the worst is 20179, and the average number of evaluations is 20385. The solution result is better than ICSA, but the computational cost is also higher. If $N=10$, $G=360$, and the results obtained by ICSA running 15 times, the best is 20375, the worst is 20186, the average number of evaluations is 18124, the average number of evaluations of ICSA is less than CACO, and the best and most The difference is better than CACO. Obviously, ICSA's comprehensive performance is stronger than CACO.

For the SCH and KUR test functions, the Pareto frontiers obtained by SPEA2 and NSGA2 are not very ideal. Although most of the results converge to the ideal Pareto frontier, the distribution of the solution is poor, and the corresponding multi-objective optimization algorithm is obtained the results of not only converge to the ideal Pareto front, but also the uniformity of the solution distribution is better. For the test functions ZDT1, SPEA2, and the results obtained by the multi-objective optimization algorithm are not much different, NSGA2 fails to converge to the ideal Pareto front. For the test functions ZDT2 and ZDT3, in terms of solution convergence, all three algorithms can converge to the ideal Pareto front, but the uniformity of the distribution of the solutions obtained by SPEA2 and NSGA2 is still not as good as the multi-objective optimization algorithm. For the test function ZDT6, the advantages of the multi-objective optimization algorithm are more obvious, not only in the convergence of the algorithm, but also in the uniformity of the distribution of the results obtained than SPEA2 and NSGA2. Due to the large difference in the dimensions of the values participating in the training, for the operability and training accuracy of the training, we perform input normalization operations on the samples participating in the training, and then perform training to obtain the corresponding multi-objective

optimization algorithm model. In the same way, after obtaining the multi-objective optimization algorithm model, we also need to perform the output denormalization operation on the corresponding output value to obtain the value in line with the dimension. Combining the above analysis, we use the multi-objective optimization algorithm model to approximate the system model. The comparison between the learning output value of the multi-objective optimization algorithm model and the corresponding actual output value and the relative error of the corresponding output value are shown in Figure 4. It can be seen from the figure that the trained RBF neural network approximates the system model very well, and its error is controlled within a certain range (1×10^{-3}), so it meets our design requirements. But in order to further test the feasibility of the multi-objective optimization algorithm model, we take another 30 sets of actual values that have not participated in the training to make predictions, and compare them with the actual values. The output of the multi-objective optimization algorithm model is still close to the output of the corresponding actual value, and its error is still controlled within a certain range (1×10^{-3}), so it meets our requirements. Based on the above description, it is feasible to replace the Aspenplus mechanism model with the system multi-objective optimization algorithm model obtained through training.

V. CONCLUSION

Artificial immune algorithm is a learning algorithm based on the biological immune system. It has excellent system autonomy and responsiveness, and has the function of optimizing retrieval. This algorithm combines knowledge of statistical immunology and evolutionary algorithms, and has attracted much attention. In the multifunctional evolutionary algorithm based on aggregation density, the aggregation density is introduced into the algorithm, and the Pareto optimal solution set is updated to obtain the optimal solution set. According to the characteristics of these two algorithms, this research will improve and innovate the algorithm and apply the new algorithm to image analysis problems.

The artificial immune algorithm is mainly based on the simplified mechanism of the immune system to design optimization algorithms, and to solve engineering problems through the supplement of related technologies. In particular, the constrained optimization immune algorithm reflects the possibility of developing algorithms that use immune mechanisms to deal with constrained optimization problems. Secondly, by combining fuzzy rules and immune mechanisms to design multi-objective control immune algorithms, fuzzy rules play a great auxiliary role in the design of optimization algorithms with dynamic characteristics, which is a research topic that hides huge possibilities. Finally, in order to understand the difference between the neural network and the immune algorithm in the optimization problem, the neural network is proposed, and the theoretical research and comparison are carried out.

This research theoretically analyzes the general multi-objective optimization algorithm, and provides sufficient

conditions for the convergence of this multi-objective optimization algorithm. In addition, using the general GA algorithm, analyze the random convergence characteristics of the multi-objective optimization algorithm under the action of a simple hyperstatic algorithm, that is, to ensure the upper limit of the evolutionary algebra required for the next step. This is the overall best solution under fixed probability development and is compared with GA. These theoretical analyses and comparisons are of great importance to the theoretical research of multi-objective optimization algorithms. Of course, for the complexity analysis of specific types of optimization problems, more research is needed.

REFERENCES

- [1] Z. Libo, H. Tian, G. Chunyun, and M. Elhoseny, "Real-time detection of cole diseases and insect pests in wireless sensor networks," *J. Intell. Fuzzy Syst.*, vol. 37, no. 16, pp. 1–12, 2019.
- [2] M. Abdel-Basset, M. El-Hoseny, A. Gamal, and F. Smarandache, "A novel model for evaluation hospital medical care systems based on plithogenic sets," *Artif. Intell. Med.*, vol. 100, Sep. 2019, Art. no. 101710.
- [3] A. F. S. Devaraj, M. Elhoseny, S. Dhanasekaran, E. L. Lydia, and K. Shankar, "Hybridization of firefly and improved multi-objective particle swarm optimization algorithm for energy efficient load balancing in cloud computing environments," *J. Parallel Distrib. Comput.*, vol. 142, pp. 36–45, Aug. 2020.
- [4] Z. Lv and N. Kumar, "Software defined solutions for sensors in 6G/IoE," *Comput. Commun.*, vol. 153, pp. 42–47, Mar. 2020.
- [5] Y. Lou, J. Shi, D. Guo, A. K. Qureshi, and L. Song, "Function of PD-L1 in antitumor immunity of glioma cells," *Saudi J. Biol. Sci.*, vol. 24, no. 4, pp. 803–807, May 2017.
- [6] R. Saileela et al., "Causality, information and biological computation: An algorithmic software approach to life, disease and the immune system," *Computer*, vol. 3, no. 3, pp. 399–401, 2016.
- [7] M. Elhoseny, A. Shehab, and X. Yuan, "Optimizing robot path in dynamic environments using genetic algorithm and bezier curve," *J. Intell. Fuzzy Syst.*, vol. 33, no. 4, pp. 2305–2316, Sep. 2017.
- [8] S. Qian, Y. Ye, B. Jiang, and J. Wang, "Constrained multiobjective optimization algorithm based on immune system model," *IEEE Trans. Cybern.*, vol. 46, no. 9, pp. 2056–2069, Sep. 2016.
- [9] M. Yu, Y. Dong, and Y. Takeuchi, "Dual role of delay effects in a tumour-immune system," *J. Biol. Dyn.*, vol. 11, no. 2, pp. 334–347, Aug. 2017.
- [10] P. Saurabh and B. Verma, "An efficient proactive artificial immune system based anomaly detection and prevention system," *Expert Syst. Appl.*, vol. 60, pp. 311–320, Oct. 2016.
- [11] B. S. Murugan, M. Elhoseny, K. Shankar, and J. Uthayakumar, "Region-based scalable smart system for anomaly detection in pedestrian walkways," *Comput. Electr. Eng.*, vol. 75, pp. 146–160, May 2019.
- [12] Z. Ning, X. Mengjue, M. Weijian, "Modeling and solution for inbound container storage assignment problem in dual cycling mode," *Transp. Res. E, Logistics Transp. Rev.*, vol. 79, pp. 49–64, 2018.
- [13] Y. Zhang, H. Huang, L.-X. Yang, Y. Xiang, and M. Li, "Serious challenges and potential solutions for the industrial Internet of Things with edge intelligence," *IEEE Netw.*, vol. 33, no. 5, pp. 41–45, Sep. 2019.
- [14] T. Wei and M. Tang, "Biological effects of airborne fine particulate matter (PM_{2.5}) exposure on pulmonary immune system," *Environ. Toxicol. Pharmacol.*, vol. 60, pp. 195–201, Jun. 2018.
- [15] E. I. Finkina, D. N. Melnikova, I. V. Bogdanov, and T. V. Ovchinnikova, "Peptides of the innate immune system of plants. Part I. Structure, biological activity, and mechanisms of action," *Russian J. Bioorganic Chem.*, vol. 44, no. 6, pp. 573–585, Nov. 2018.
- [16] R. H. Hameed, "Psychological and biological effects of stress on human immune system," *Indian J. Public Health Res. Develop.*, vol. 9, no. 8, p. 1233, 2018.
- [17] B. Zhu, R. Pang, J. Chevallier, Y.-M. Wei, and D.-T. Vo, "Including intangible costs into the cost-of-illness approach: A method refinement illustrated based on the PM_{2.5} economic burden in China," *Eur. J. Health Econ.*, vol. 20, no. 4, pp. 501–511, Jun. 2019.

- [18] J. T. Instanes, A. Halmøy, A. Engeland, J. Haavik, K. Furu, and K. Klungsoyr, "Attention-deficit/hyperactivity disorder in offspring of mothers with inflammatory and immune system diseases," *Biol. Psychiatry*, vol. 81, no. 5, p. 452, 2017.
- [19] N. Cattane, C. Mora, N. Mariani, M. A. Riva, C. M. Pariante, and A. Cattaneo, "T200. MiRNA-19 as a key player in the modulation of the immune system and neuroplasticity during neurodevelopment: Impact on the risk for psychosis," *Biol. Psychiatry*, vol. 83, no. 9, p. S206, May 2018.
- [20] A. Larange and H. Cheroutre, "Retinoic acid and retinoic acid receptors as pleiotropic modulators of the immune system," *Annu. Rev. Immunol.*, vol. 34, no. 1, pp. 369–394, May 2016.
- [21] K. Geetha, V. Anitha, M. Elhoseny, S. Kathiresan, P. Shamsolmoali, and M. M. Selim, "An evolutionary lion optimization algorithm-based image compression technique for biomedical applications," *Expert Syst.*, Jan. 2020, Art. no. e12508.
- [22] L. Fabisiak, "Web service usability analysis based on user preferences," *J. Org. End User Comput.*, vol. 30, no. 4, pp. 1–13, Oct. 2018.
- [23] M. K. Trivedi, M. Gangwar, S. C. Mondal, and S. Jana, "Role of vital trace elements in nanocurcumin-centered formulation: A novel approach to resuscitate the immune system," *Biol. Trace Element Res.*, vol. 182, no. 2, pp. 265–277, Apr. 2018.
- [24] E. M. Frans, "The importance of immune system diseases in the etiology of attention-deficit/hyperactivity disorder," *Biol. Psychiatry*, vol. 81, no. 5, pp. e39–e40, Mar. 2017.
- [25] S. Mnif, S. Darmoul, S. Elkosantini, and L. B. Said, "An immune multi-agent system to monitor and control public bus transportation systems," *Comput. Intell.*, vol. 34, no. 4, pp. 1245–1276, Nov. 2018.
- [26] M. Eshete, K. Bailey, T. D. T. Nguyen, S. Aryal, and S.-O. Choi, "Interaction of immune system protein with PEGylated and un-PEGylated polymeric nanoparticles," *Adv. Nanoparticles*, vol. 6, no. 3, pp. 103–113, 2017.
- [27] B.-K. Yoo, K. Kwon, Y. H. Ko, H. G. Kim, S. Lee, K.-H. Park, J.-Y. Choi, and O.-Y. Kwon, "Screening of natural product libraries for the extension of cell life-span through immune system," *J. Life Sci.*, vol. 26, no. 3, pp. 359–363, Mar. 2016.
- [28] C. Wen, R. C. Seeger, M. Fabbri, L. Wang, A. S. Wayne, and A. Y. Jong, "Biological roles and potential applications of immune cell-derived extracellular vesicles," *J. Extracellular Vesicles*, vol. 6, no. 1, Dec. 2017, Art. no. 1400370.
- [29] Z. Lv and L. Qiao, "Deep belief network and linear perceptron based cognitive computing for collaborative robots," *Appl. Soft Comput.*, vol. 92, Jul. 2020, Art. no. 106300.
- [30] R. Paganelli, C. Petrarca, and M. Di Gioacchino, "Biological clocks: Their relevance to immune-allergic diseases," *Clin. Mol. Allergy*, vol. 16, no. 1, p. 1, Dec. 2018.
- [31] H. Ayaydin, O. Abali, N. O. Akdeniz, B. E. Kok, A. Gunes, A. Yildirim, and G. Deniz, "Immune system changes after sexual abuse in adolescents," *Pediatrics Int. Off. J. Japan Pediatric Soc.*, vol. 58, no. 2, pp. 105–112, Feb. 2016.
- [32] I. Gálvez, S. Torres-Piles, and E. Ortega-Rincón, "Balneotherapy, immune system, and stress response: A hormetic strategy?" *Int. J. Mol. Sci.*, vol. 19, no. 6, p. 1687, Jun. 2018.
- [33] A. Halaris, "Modulation of immune system activation may arrest neuroprogression in bipolar disorder," *Biol. Psychiatry*, vol. 81, no. 10, p. S314, May 2017.
- [34] M. Galeas-Pena, N. McLaughlin, and D. Pociask, "The role of the innate immune system on pulmonary infections," *Biol. Chem.*, vol. 400, no. 4, pp. 443–456, Apr. 2019.
- [35] M. H. Nurtudinovich, P. K. Khristoforovich, M. G. Harisovna, C. A. Nikolaevich, S. G. Nikolaevich, V. N. Mikhailovich, and F. T. Hadievich, "Condition of immune system of the fruit and possibility of vaccinal prevention of infectious diseases of young growth of the early postnatal period," *Res. J. Pharmaceutical, Biol. Chem. Sci.*, vol. 7, no. 4, pp. 2200–2206, 2016.
- [36] Z. Lv, X. Li, and W. Li, "Virtual reality geographical interactive scene semantics research for immersive geography learning," *Neurocomputing*, vol. 254, pp. 71–78, Sep. 2017.
- [37] Y. Ding, N. Xu, S. Dai, L. Ren, K. Hao, and B. Huang, "An immune system-inspired reconfigurable controller," *IEEE Trans. Control Syst. Technol.*, vol. 24, no. 5, pp. 1–8, Sep. 2016.
- [38] B. Pawłowski, J. Nowak, B. Borkowska, D. Augustyniak, and Z. Drulis-Kawa, "Body height and immune efficacy: Testing body stature as a signal of biological quality," *Proc. Roy. Soc. B, Biol. Sci.*, vol. 284, no. 1859, Jul. 2017, Art. no. 20171372.
- [39] E. Alizadeh, N. Meskin, and K. Khorasani, "A negative selection immune system inspired methodology for fault diagnosis of wind turbines," *IEEE Trans. Cybern.*, vol. 47, no. 11, pp. 3799–3813, Nov. 2017.
- [40] Z. Lv, "Virtual reality in the context of Internet of Things," *Neural Comput. Appl.*, vol. 32, pp. 1–10, Sep. 2019.
- [41] M. C. A. Prado and C. Rodríguez-Padilla, "Role of the immune system in the microenvironment of malignant tumors of breast," *Revista Cubana de Hematología, Inmunología y Hemoterapia*, vol. 32, no. 2, pp. 190–202, 2016.
- [42] J. Shi, X. Fei, L. Yajing, Y. Ting, G. Ying, M. Li, and L. Letao, "Active distribution system planning for low-carbon objective using immune binary firefly algorithm," *J. Tianjin Univ.*, vol. 50, no. 5, pp. 507–513, 2017.



JUAN BAO was born in Shiyan, Hubei, China, in 1983. She received the bachelor's degree from the Wuhan University of Technology, China, the master's degree from the Wuhan University of Science and Technology, and the Ph.D. degree from the Wuhan University of Technology. She is currently working with the School of Public Health, Hubei University of Medicine. Her research interests include information engineering, and control and emergency management.



XIANGYANG LIU was born in Jingmen, Hubei, China, in 1980. He received the bachelor's degree from Hubei University, China, and the master's degree from the East China University of Technology, China. He is currently pursuing with the School of Public Health, Hubei University of Medicine. His research interests include machine learning and data mining.



ZHENGTAO XIANG was born in Yuanan, Hubei, China, in 1974. He received the bachelor's degree from the Hubei University of Automotive Technology, China, in 1997, the master's degree from Zhejiang University, China, in 2004, and the Ph.D. degree from Shanghai University, China, in 2013. He is currently working with the School of Electrical and Information Engineering, Hubei University of Automotive Technology. His research interests include computer networks and traffic flow modeling.



GANG WEI was born in Xiaogan, Hubei, China, in 1979. He received the bachelor's degree from the Hubei University of Medicine, China, and the master's degree from Wuhan University, China. He is currently working with The Affiliated People's Hospital of Hubei University of Medicine. His research interests include medical teaching and scientific research of digestive diseases.